

Correlated Polaron Transport and Magnetoresistance in Sol-Gel Prepared $\text{La}_{0.7}\text{Sr}_{0.3-x}\text{Ca}_x\text{MnO}_3$ ($x = 0.1, 0.15, 0.2$) Nanomanganite System

U. L. Shinde¹, N. B. Srivastava², L. N. Singh³

¹*K. J. Somaiya Institute of Engineering & IT, Sion(E), Mumbai-400022, India*

²*Department of Physics, R. Jhunjhunwala College, Ghatkopar, Mumbai, India*

³*Dr. Babasaheb Ambedkar Technological University, Lonere, Raigad, India*

¹ushinde@somaiya.edu

Abstract-Transport behavior and magnetoresistance in sol-gel prepared $\text{La}_{0.7}\text{Sr}_{0.3-x}\text{Ca}_x\text{MnO}_3$ ($x = 0.1, 0.15, 0.2$) nanomanganite system have been investigated in the temperature range 10 – 400 K. It is found that with increase in Ca^{2+} ion concentration metal-insulator transition temperature (T_{MI}) decreases and on the application of magnetic field T_{MI} shift toward higher temperature with decrease in resistivity. It is shown that the correlated polaron model accounts for the temperature dependence of resistivity in the entire temperature range.

Keywords: CMR, XRD, SEM, Nanomanganites, Polaron, Magnetoresistance

I. INTRODUCTION

Perovskite manganites with the general formula $\text{Ln}_{1-x}\text{A}_x\text{MnO}_3$ ($\text{Ln} = \text{La, Pr, Nd}$; $\text{A} = \text{Ca, Sr, Ba}$) have been the subject matter of significant research due to their unusual colossal magnetoresistance (CMR) property along with interesting electrical and magnetic properties [1, 2]. The phenomenon of CMR observed in doped manganites is not yet fully understood despite of numerous attempts. It is also reported that nanocrystalline manganites have higher magnitude of the low field magnetoresistance as compare to ceramic samples [3]. They have also potential applications for magnetic recording, memory storage and magnetic sensors [4]. It has been shown that average A site cation radius $\langle r_{\text{A}} \rangle$ (equivalent to the perovskite tolerance factor $\tau = (\langle r_{\text{A}} \rangle + r_{\text{O}}) / \sqrt{2}(r_{\text{B}} + r_{\text{O}})$) and related parameters like A site cation size variance $\sigma^2 \langle r_{\text{A}} \rangle = \sum y_i r_i^2 - \langle r_{\text{A}} \rangle^2$ influences the behavior of resistivity with temperature in manganites [5, 6]. Therefore an effort has been made to correlate T_{MI} with above parameters by substituting different cations at A site.

The synchronized occurrence of ferromagnetism and metallic nature in the low temperature region ($T < T_{\text{MI}}$) qualifies it to be one of the most remarkable physical properties of these materials. Zener's double exchange model is the widely proposed mechanism [7], in which the electronic conduction is connected to ferromagnetic interaction between Mn^{3+} and Mn^{4+} via intermediate oxygen atom. Due to its inability to interact with the spin–lattice or charge–lattice

interactions, i.e. Jahn–Teller (JT) interaction and polarons, that significantly contributes to very large resistivity in the paramagnetic insulating phase [8, 9], it is considered to be a major drawback. There is thus a need to understand the electrical conduction in terms of correlation effects in polaronic transport. Sol–gel routes produce very high quality, homogeneous and fine particle samples [10– 12]. Here, we report the synthesis of $\text{La}_{0.7}\text{Sr}_{0.3-x}\text{Ca}_x\text{MnO}_3$ ($x = 0.1, 0.15, 0.2$) using sol-gel technique. Structural and electrical properties of nanomanganite have been presented.

II. EXPERIMENTAL

$\text{La}_{0.7}\text{Sr}_{0.3-x}\text{Ca}_x\text{MnO}_3$ ($x = 0.1, 0.15, 0.2$) manganites have been prepared by sol-gel process using metal chlorides (Aidrich made) as starting materials. In this process the stoichiometric amount of metal chlorides in the form of solution were converted into citrates and pH was adjusted between 2 to 3. After getting sol on slow evaporation, a gelating reagent ethylene glycol was added and heated around 100 °C to get a gel. The gel on further heating in oven at 200 °C around 12 hours yields a dry fluffy porous mass, which was calcined at 800 °C for 2 hours. Then the powders were pressed into circular pellets and were sintered at 1000 °C in air for 4 hours. All the materials are characterized by X-ray diffraction (XRD) using BRUKER DIFRACTOMETER with Cu anode (Cu K α radiation source $\lambda = 1.5410 \text{ \AA}$) at room temperature, by collecting the data in 2θ range of 20° - 80°. Scanning Electron Microscope (SEM) studies (on Hitachi s-4800 2nd type) were performed to examine the surface morphology of the samples along with the energy dispersive X-ray analysis (EDS) study for elemental analysis. To obtain the metal insulator transition temperature T_{MI} and to investigate the influence of magnetic field on the transport behavior of these samples ($\text{La}_{0.7}\text{Sr}_{0.2}\text{Ca}_{0.1}\text{MnO}_3$, $\text{La}_{0.7}\text{Sr}_{0.15}\text{Ca}_{0.15}\text{MnO}_3$ and $\text{La}_{0.7}\text{Sr}_{0.1}\text{Ca}_{0.2}\text{MnO}_3$), electrical resistance was measured using Quantum design PPMS over temperature range 10 - 400 K at applied magnetic field 0 and 2 T. In case of sample $\text{La}_{0.7}\text{Sr}_{0.15}\text{Ca}_{0.15}\text{MnO}_3$, variation of resistivity with the

temperature is measured at applied magnetic field 0 and 0.5 T in the range 10 - 330 K.

III. RESULTS AND DISCUSSION

A) X-ray and SEM analysis

The X-ray diffraction patterns of the samples are shown in Fig. 1. The X-ray diffraction pattern clearly reveals that all the samples have a perovskite orthorhombic structure. The average crystallite size value have been calculated based on full width at the half maxima of the XRD peaks by using Scherrer formula [13]

$$\langle D \rangle = \frac{K\lambda}{\beta \cos \theta} \tag{1}$$

Where K is constant (K = 0.9), λ is the wavelength of Cu K α radiation ($\lambda = 1.541 \text{ \AA}$) and β is full width of half maxima of XRD peak. The calculated values of $\langle D \rangle$ for all the samples are found to be 30 to 36 nm range and given in table I. Fig. 2 shows SEM images of the samples. The fluffy nature and voids in solgel derived powder can be attributed to large amount of gases evolved during reaction.

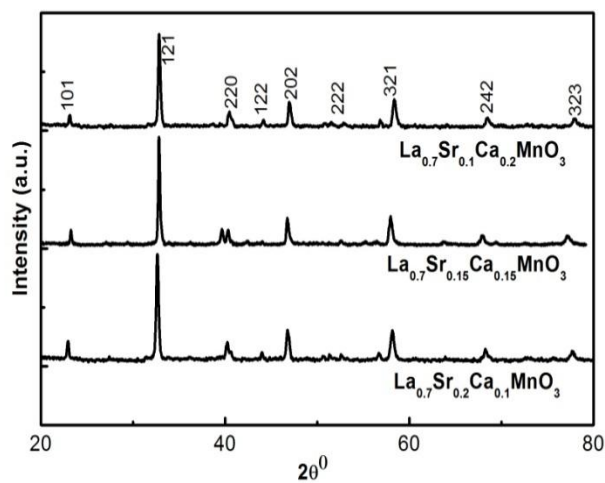


Fig. 1 : X-ray diffraction patterns of the series $\text{La}_{0.7}\text{Sr}_{0.3-x}\text{Ca}_x\text{MnO}_3$ ($x = 0.1, 0.15, 0.2$)

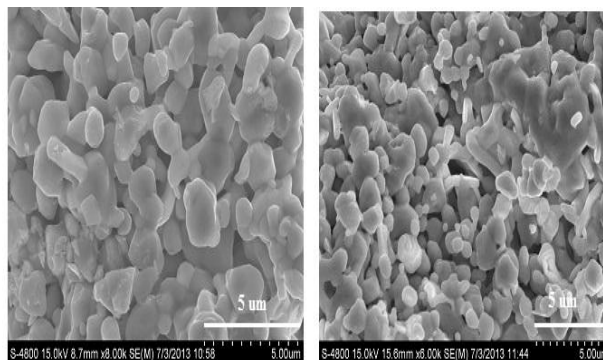


Fig. 2. SEM images of samples $\text{La}_{0.7}\text{Sr}_{0.3-x}\text{Ca}_x\text{MnO}_3$ ($x = 0.1, 0.2$)

B) Effect of cation substitution at A site on magnetotransport properties of manganites

It has been shown that metal insulator transition temperature (T_{MI}) of manganites is controlled by the average A site cation radius and by varying the oxygen content. It has been established that T_{MI} increases with size variance, $\sigma^2 \langle r_A \rangle$ and vice versa [5, 6].

Therefore to understand the effect of variation of A site ionic radii $\langle r_A \rangle$ and size variance, $\sigma^2 \langle r_A \rangle$ on magnetotransport properties of La based manganites, the average A site ionic radii and size variance have been calculated using the coordination number twelve [14] and are given in table I. The values of metal-insulator transition temperature of all samples are given in table I. The variation of resistivity with temperature in absence and presence of magnetic field is shown in Fig. 3. It is interesting to note that T_{MI} increases thereafter with $\sigma^2 \langle r_A \rangle$. This variation is shown in figure Fig. 4a. This type of behavior is in contrast with the normally observed by several manganites [15, 16]. The reason for the unusual behavior exhibited by the samples could be explained on the basis of size mismatch at A site. It is observed that as Sr^{2+} content decrease resistivity increase in Ca^{2+} substituted samples. It may be due to the partial substitution of Ca^{2+} ions onto Sr^{2+} ions, which reduces the value of $\langle r_A \rangle$. Due to this A-O and Mn-O bond distance decrease which results in more pronounced lattice distortion and hence localization of e_g electrons. Moreover the transfer integral (t) of the e_g electrons hopping from Mn^{3+} to Mn^{4+} , defined as $t = t_0 \cos(\theta/2)$ [17] (where t_0 is the normal transfer integral and θ is the angle between two neighboring spin directions) reduces more drastically in the case of Ca substituted compounds. This leads to suppression of the DE interaction between the Mn^{3+} and Mn^{4+} and to increase in resistivity values in Ca substituted compounds. This effect results in the decrease of T_{MI} with increasing Ca^{2+} ion substitution onto Sr^{2+} ion.

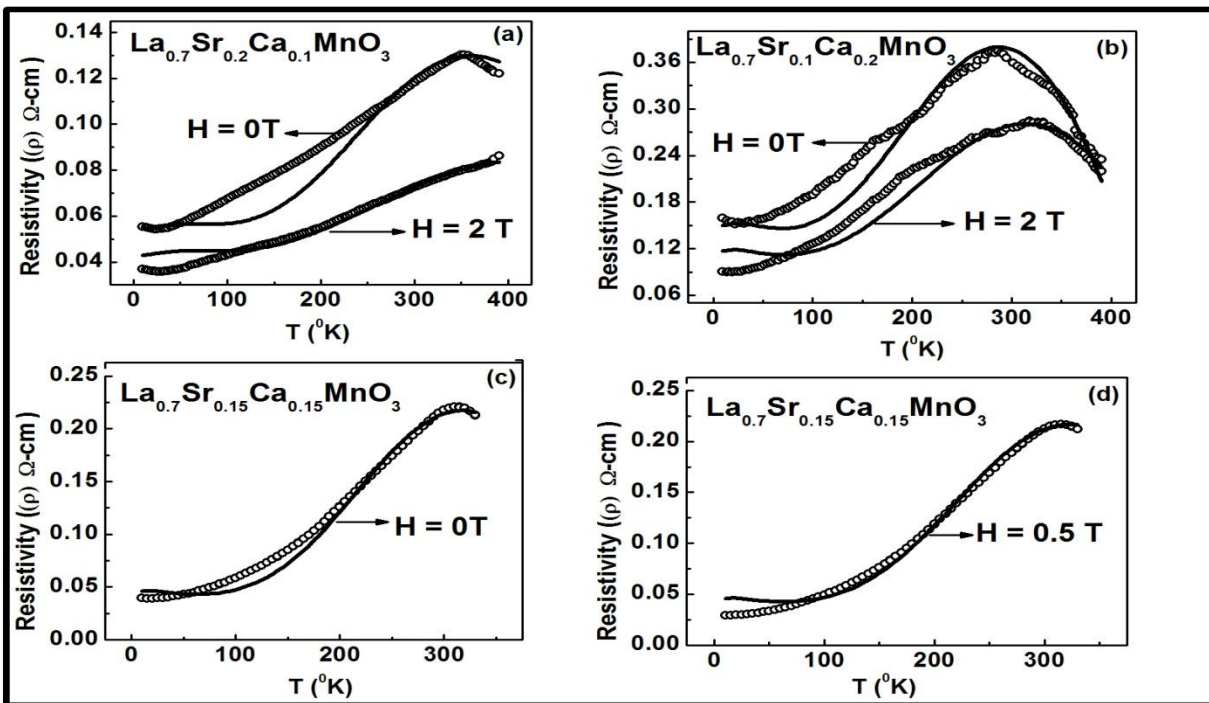


Fig. 3(a-d): Observed variation of resistivity with temperature in absence and presence of magnetic field for $\text{La}_{0.7}\text{Sr}_{0.3-x}\text{Ca}_x\text{MnO}_3$ ($x = 0.1, 0.15, 0.2$). The experimental points are shown in hollow circles. The fitted plots are shown by solid lines using Eq. (5) with parameters given in Table II.

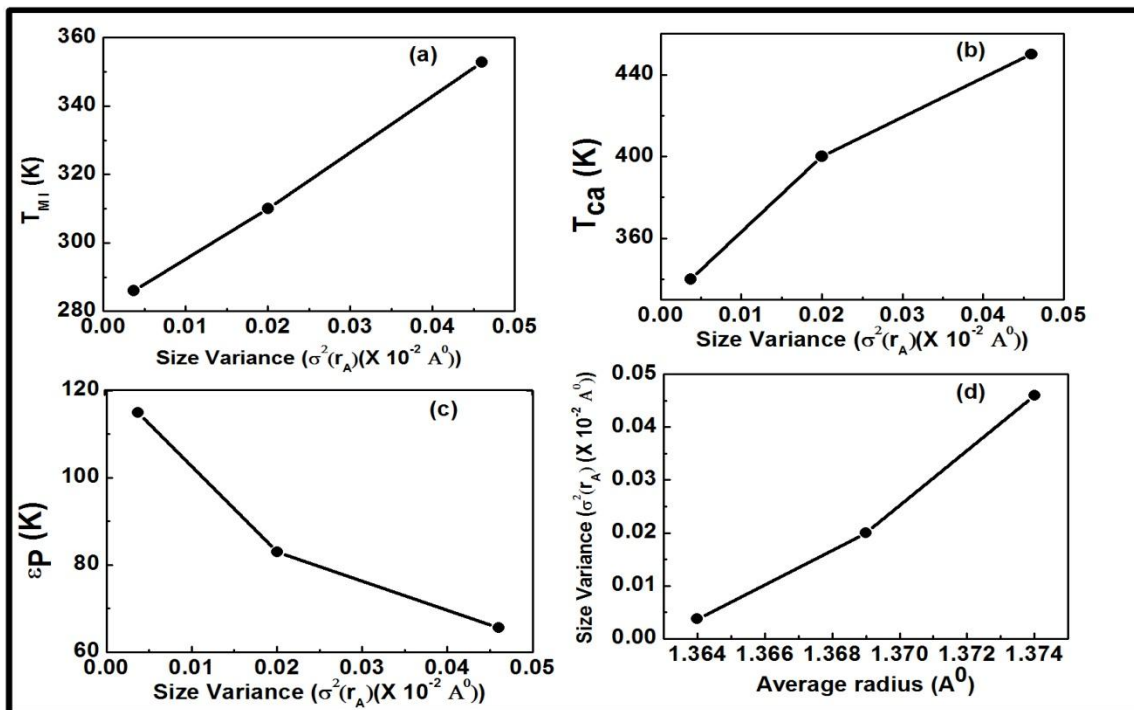


Fig. 4(a-d): Variation of T_{Mi} , T_{Ca} , and ϵP with size variance $\sigma^2\langle r_A \rangle$ (from Table I and II.)

TABLE I: EXPERIMENTAL DATA OF LANTHANUM MANGANITES

Sample	$\langle D \rangle$ nm	$\langle r_A \rangle$ Å	$\sigma^2 (r_A)$ ($\times 10^{-2}$ Å ²)	τ	T_{MI} (K)		ρ_{MI} (Ωcm)	MR%
					0 T	2 T		
$\text{La}_{0.7}\text{Sr}_{0.2}\text{Ca}_{0.1}\text{MnO}_3$	35.5	1.374	0.046	0.9825	352.8	----	0.1298	36.5
$\text{La}_{0.7}\text{Sr}_{0.15}\text{Ca}_{0.15}\text{MnO}_3$	36.5	1.369	0.02	0.9807	310	315 (H = 0.5 T)	0.2207	1.67
$\text{La}_{0.7}\text{Sr}_{0.1}\text{Ca}_{0.2}\text{MnO}_3$	31.2	1.364	0.0037	0.9789	286	318	0.2846	25

C) Conduction Mechanism

We show in this paper that the Correlated Polaron (CP) model proposed by Srivastava[18] gives satisfactory account of the variation of resistivity curve with temperature. The CP model is based on the Holstein Hamiltonian for a molecular crystal in which a charge carrier is shared between two atoms. In this model the electron itinerancy is promoted by valance exchange (VE) in mixed valance ionic compounds. In systems with an anion or a cation in mixed valance state on crystallographic equivalent sites, there are two possible ways to arrange the ions, that can be represented by degeneracy states in static lattices but on coupling to the longitudinal optics phonons the degeneracy is removed. The conductivity is given by [19]

$$\sigma_{hop} = (\sqrt{\pi}/2)n(t/h)^2 e^2 a^2 (\tau/k_B T) \text{sech}^2(\varepsilon_p / 2k_B T) \exp(-U / k_B T) \quad (2)$$

Here n is the no. of polarons, a is the separation between the sites two which the electron hopes, $t = \langle t_{ij} \rangle$ is the average hopping amplitude, τ is the relaxation time, and U is the activation energy, ε_p is the small polarization stabilization energy and e, h, k_B are the electron charge, Plank constant and Boltzmann constant respectively. sech term arises from the average no. of electrons at the initial site i and the average no of holes at site j in the jump process. The mobility is govern by the Einstein relation $\mu = eD/k_B T$ with the diffusion constant $D = a^2 v_{ph}$. In the CP model that applies to mixed valance compound like $\text{Ln}_{1-x}\text{A}_x\text{Mn}_{1-x}^{3+}\text{Mn}_x^{4+}\text{O}_3$ the valance exchange ($\text{Mn}^{4+}\text{Mn}^{3+} \leftrightarrow \text{Mn}^{3+}\text{Mn}^{4+}$) takes place and the following relation holds [18]

$$1/\tau = v_{ph}[1 + c(1-m^2)\sigma_a^2] \quad (3a)$$

$$U = U_0(1-m^k)\sigma_a^2 \quad (3b)$$

$$m(t_c) = M(T)/M(T_c), \quad t_c = T/T_c(3c)$$

$$\sigma_a = (1 - 0.75 t_{ca}^3)^{1/2}, \quad t_{ca} = T/T_{ca} \quad (3d)$$

Here m is reduced magnetization given by Brillouin function for spin $j=1/2$, T_C is the Curie temperature and σ_a is atomic order parameter. T_{ca} denotes order-disorder crossover temperature of a binary alloy $\text{Mn}_{1-x}^{3+}\text{Mn}_x^{4+}$, c is the constant arising from low temperature spin wave excitations and k a constant arises from the critical point magnetic excitations near T_C . The phonon frequency $v_{ph} = 5.5 \times 10^{12}$ Hz [18] is observed by Dai et al [20]. For $T < \theta_D/4$, where θ_D is Debye temperature, the zero-point lattice vibration dominates and takes the place of thermal phonon. The resistivity is then given by [18]

$$\rho(T) = \frac{A}{n} [(1-f) \frac{\theta}{4} \cosh^2(2\varepsilon_p/k_B \theta_D) + fT \cosh^2(\varepsilon_p/2k_B T)] [1 + c(1-m^2)\sigma_a^2] \exp[U/k_B T] \quad (4)$$

where, $A = 1.13k_B/a^2 e^2 v_{ph}$ and f is the polaron distribution function $\exp(\varepsilon_p/k_B T + 1)^{-1}$ between the localized and band polaron states.

The resistivity curve for $\text{La}_{0.7}\text{Sr}_{0.3-x}\text{Ca}_x\text{MnO}_3$ ($x = 0.1, 0.15, 0.2$) are compared to Eq. 4 with the parameters given in Table II and from the quality of these fittings one may conclude that this equation might be an appropriate one to explain the conduction mechanism of the samples of present investigation. In Eq. 4 the parameters θ_D was taken as 425 K, ε_p was varied till the best fit was obtained. T_{ca} was taken from the best fit of the paramagnetic part $\rho(T > T_C)$ of the curve. c and k were nearly constant. U_0 again was taken constant as 580 K for the best fit. The best fit parameters T_{ca} and ε_p for all the samples are presented in Table II and plots are shown in Fig. 3. The Debye temperature is 425 K in all the cases. Further, all the three parameters T_{ca} , ε_p and U_0 in the presence of magnetic field, have also been computed for all the materials and are given in Table II. The parameter T_{ca} found to increase and ε_p found to decrease on the application of magnetic field whereas U_0 is nearly same. All the three parameters obtained from resistivity data has an interesting dependence on doping concentration x which indicates that T_{ca} and ε_p depends upon cation mismatch. The variation of T_{ca} and ε_p is shown in Fig. 4.

The number of charge carriers, n , increases as Sr^{2+} ion concentration increases which is responsible for the decrease in resistivity values. The small polaron binding energy, ε_p , is found to increase as Sr^{2+} ion concentration increases. The thermally assisted activation energy, U_0 , is same as the system varies from Ca- to Sr- substitution. The ε_p is related to the depth

of the potential well which localizes the electron so conductivity $\sigma \propto \text{sech}^2 [\varepsilon_p/2k_B T]$ as $T \rightarrow 0$ where zero point vibrations dominate. As expected ε_p increases as the deviation of Mn-O-Mn bond angle deviate from 180° . Therefore as Sr^{2+} ion concentration decreases ε_p increases.

TABLE II: THE BEST FIT PARAMETERS T_{ca} , ε_p and U_0 FOR ALL THE SAMPLES. THE DEBYE TEMPERATURE θ_D IS 425 K IN ALL CASES. n/x IS THE RATIO OF THE CARRIER CONCENTRATION DATA FROM Eq. (1) AND THE NOMINAL HOLE CONCENTRATION FROM COMPOSITION. THE VALUE OF N HAS BEEN OBTAINED FROM THE VALUES USING $\nu_{ph} \sim 5.5 \times 10^{12}$ Hz WITH $a = 5.4617 \text{ \AA}$.

Samples (Magnetic field in T)	T_{ca} (K)	ε_p (K)	U_0 (K)	A/n 10^4 ($\Omega\text{cm/K}$)	C	k	n/x (\times 10^{19})	n/Mn (\times 10^{-1})
$\text{La}_{0.7}\text{Sr}_{0.2}\text{Ca}_{0.1}\text{MnO}_3$ (0 T)	450	65.6	580	2.6	1	2.5	14	22.8
$\text{La}_{0.7}\text{Sr}_{0.2}\text{Ca}_{0.1}\text{MnO}_3$ (2 T)	470	60.0	580	2.4	1	2.5	15.7	25.5
$\text{La}_{0.7}\text{Sr}_{0.15}\text{Ca}_{0.15}\text{MnO}_3$ (0 T)	400	83.0	580	3.6	3	1.7	10.3	16.8
$\text{La}_{0.7}\text{Sr}_{0.15}\text{Ca}_{0.15}\text{MnO}_3$ (0.5 T)	405	80.9	580	3.6	3	1.7	10.43	17.0
$\text{La}_{0.7}\text{Sr}_{0.1}\text{Ca}_{0.2}\text{MnO}_3$ (0 T)	340	114.9	580	10.5	2	0.7	3.53	5.7
$\text{La}_{0.7}\text{Sr}_{0.1}\text{Ca}_{0.2}\text{MnO}_3$ (2 T)	360	102.5	580	8.6	1.5	0.7	4.3	7.0

D) Magnetoresistance Behavior

The variation of resistivity with temperature is shown in figure 3a-d for all the samples in the range of 10 to 400 K. It is observed from the high temperature end that resistivity increases continuously with decrease in temperature up to the metal insulator transition temperature (T_{MI}) indicated by the peak in the curve. On further decrease in temperature ρ decreases sharply. On application of the magnetic field T_{MI} moves to a higher temperature with decrease in ρ_{MI} (T_{MI}) resistivity. The observed behavior may be attributed to the fact that the applied magnetic field induces delocalization of charge carriers, which in turn suppresses the resistance causing local ordering of the magnetic spins. Hence, the transition temperature (T_{MI}) moves to a high temperature side on the application of magnetic field [16, 21, 22].

The percentage of magnetoresistance (MR) is calculated using the relation

$$\text{MR} = \frac{\rho(0) - \rho(H)}{\rho(0)} \times 100 \quad (5)$$

Where $\rho(0)$ = resistivity at zero magnetic field, $\rho(H)$ = resistivity in magnetic field 0.5 T. Magnetoresistance for all samples at T_{MI} is shown in table I. Because of the impact of replacement of Sr^{2+} ions by Ca^{2+} , the intrinsic MR increases with Ca^{2+} ion addition. Thus with decreasing $\langle r_A \rangle$ and $\sigma^2 \langle r_A \rangle$ T_{MI} decreases and MR increases.

CONCLUSIONS

In this work we have investigated structural, transport and magnetotransport properties of sol-gel prepared $\text{La}_{0.7}\text{Sr}_{0.3-x}\text{Ca}_x\text{MnO}_3$ ($x = 0.1, 0.15, 0.2$) nanomanganite. With decrease in Sr^{2+} ion concentration the resistivity increases and T_{MI} shift toward lower temperature. The results were explained in terms of cation mismatch leading to reduction of Mn-O-Mn angle that weakens the double exchange interaction. Probably for the first time it is shown that there is generally an increase in metal-insulator transition temperature and atomic order

transition temperature for transport in La based nanomanganites with increase in cation mismatch parameter. Contrary to these small polaron stabilization energy decrease sharply on cation mismatch.

REFERENCES

- [1] *Colossal Magnetoresistance Oxides*, edited by Y. Tokura (Gordon and Breach, New York, 2000)
- [2] E. Dagotto, *Nanoscale Phase Separation in Manganites* (Springer-Verlag, Heidelberg, 2002).
- [3] M. B. Salamon, M. Jaime, *Rev. Mod. Phys.* 73, 583 (2001).
- [4] T Venkatesan, R. P. Sharma, *Materials Sci. Engg.* B41, 30 (1996).
- [5] J. P. Attfield *crystal Engg.* 5 (2002) 427
- [6] T.D. Thanh, L.H. Nguyen, D.H. Manh, N.V. Chien, P.T. Phong, N.V. Khiem, L.V. Hong, N.X. Phuc, *Physica B* 407, 145 (2012).
- [7] C. Zener, *Phys. Rev.* 82 (1951) 403.
- [8] S. Uhlenbruck, R. Teipen, R. Klingeler, B. Büchner, O. Friedt, M. Hücker, *Phys. Rev. Lett.* 82, 185 (1999).
- [9] A.P. Ramirez, *J. Phys.: Condens. Matter* 9 (1997) 8171.
- [10] M. Kakihana, *J. Sol-Gel Technol.* 6, 7 (1996).
- [11] L.E. Hueso, J. Rivas, F. Rivadulla, M.A. Lopez-Quintela, *J. Appl. Phys.* 86, 3881 (1999).
- [12] J. Rivas, L.E. Hueso, A. Fondado, F. Rivadulla, M.A. Lopez-Quintela, *J. Magn. Magn. Mater.* 221, 57 (2000).
- [13] B. D. Cullity, *Elements of X-ray Diffraction*, Addison-Wesley publication Co. 1997
- [14] R.D. Shannon, *Acta Cryst. A* 32 (1976) 751.
- [15] F. Damay, A. Maignan, C. Martin and B. Raveau, *J. Appl. Phys.* 81 (1997) 1372.
- [16] G. Venkataiah, P. Venugopal Reddy, *Solid State Commun.* 136 (2005) 114–119
- [17] J.M.D. Coey, *Adv. in Phys.*, 48 (1999) 167.
- [18] C.M. Srivastava, *J. Phys.: Condens. Matter* 11 (1999) 4539.
- [19] H. G. Reik in 'Polarons in ionic crystals and polar semiconductors' edited by J T Derve (North- Holland Amsterdam, 1972) 679-714
- [20] P. Dai, H. Y. Hwang, J. Zhang, J. A. Fernandez-Baca, S.-W. Cheong, C. Kloc, Y. Tomioka and Y. Tokura *Phys. Rev. B* 61, 9553(2000)
- [21] A. Banerjee, S. Pal, B.K. Chaudhuri, *J. Chem. Phys.* 115 (2001)1550.
- [22] A. Banerjee, S. Pal, S. Bhattacharya and B. K. Chaudhuri, *J Appl. Phys.* 91 (2002) 5125